

## **Synthetic VSP in frequency-independent Q media**

*Zhiming Li*

### **Abstract**

This paper presents an algorithm for calculating Synthetic Vertical Seismic Profiles (SVSP) in layered media with frequency independent  $Q$ . The effects of attenuation and dispersion are also discussed.

### **Introduction**

SVSP has played an important part in solving the inverse problem of field VSP data. By iteratively comparing the field VSP data with the SVSP and recursively adjusting the parameters used in SVSP modeling, one can not only obtain the structural information, but also improve the estimates of rock velocities and attenuation factors, as well as seismic noise.

SVSP can be constructed analytically if the following two assumptions are satisfied: (1) vertical incident wave; (2) horizontally layered media. To calculate SVSP with a non-vertical incident wave (wide angle VSP), or SVSP of a medium with dipping layers, numerical ray tracing and other algorithms are needed. This paper will discuss only the models with normal incident wave and flat layers. The wave relation between any two layers in such a model can be represented by a transport matrix equation.

The validity of regarding the quality factor,  $Q$ , as being frequency-independent, and the other physical aspects of the modeling, are discussed first.

### Physics of the model

The quality factor,  $Q$ , which characterizes a rock's absorption of seismic waves, is defined by (O'Connell and Budiansky, 1978)

$$Q = 4\pi \frac{W}{\Delta W}, \quad (1)$$

where  $W$  is average energy stored per cycle of vibration,  $\Delta W$  the energy loss per cycle. O'Connell and Budiansky (1978) also defined the relation between  $Q$  and the "loss angle",  $\varphi$ , as

$$\varphi = \tan^{-1} \frac{1}{Q}, \quad (2)$$

where  $\varphi$  is the phase angle by which the strain lags behind the stress.

The stress-strain relationship in a linearly viscoelastic material is given as (Boltzmann, 1876)

$$\sigma(t) = m(t) * \varepsilon(t) = \int_0^t \varepsilon(t-\tau) m(\tau) d\tau, \quad (3)$$

$$\varepsilon(t) = s(t) * \sigma(t) = \int_0^t \sigma(t-\tau) s(\tau) d\tau, \quad (4)$$

where  $\sigma(t)$  is the stress,  $\varepsilon(t)$  the strain,  $m(t)$  and  $s(t)$  are the inverse Fourier transforms of the viscoelastic modulus and compliance, respectively.

When a unit Heaviside step function,  $H(t)$ , is used as the strain in (3),  $\sigma(t)$  becomes the relaxation function and  $m(t)$  is the derivative of the relaxation function. On the other hand, when  $H(t)$  is used as the stress in (4),  $\varepsilon(t)$  becomes the creep function and  $s(t)$  is the derivative of the creep function.

Because creep functions usually can be regarded as proportional to a power of time  $t$ , Kjartansson (1979) used the following form as the creep function

$$\Phi(t) = \frac{1}{M_0 \Gamma(1+2\gamma)} \left( \frac{t}{t_0} \right)^{2\gamma} H(t), \quad (5)$$

where  $M_0$ ,  $\Gamma(1+2\gamma)$ , and  $t_0$  are scaling factors.  $\gamma$  is a constant determined by the properties of the material. By relating equations (2), (3), (4) and (5),  $Q$  can be represented as (Kjartansson, 1979)

$$\frac{1}{Q} = \tan(\pi\gamma). \quad (6)$$

Because  $\gamma$  is a constant, equation (6) shows  $Q$  as being frequency-independent.

This derivation of frequency-independent  $Q$  has some restrictions because of the approximation of the creep function. It has been observed that  $Q$  is frequency-dependent over either very low or very high frequency ranges. Other factors, such as rock saturation, pore pressure, confining pressure, and temperature, may also cause  $Q$  to be frequency-dependent.

However, many experiments have shown that  $Q$  is nearly constant over the seismic frequency band, 10-100 Hz (White, 1965). Figure 1 (a) shows the measured  $Q$ 's of dry and of partially saturated Massilon sandstone. Figure 1 (b) depicts the  $Q$ 's of vycor porous glass. The curves show  $Q$  to be nearly constant over the seismic frequency band. Therefore, the frequency-independent  $Q$  model will be used in our SVSP modeling.

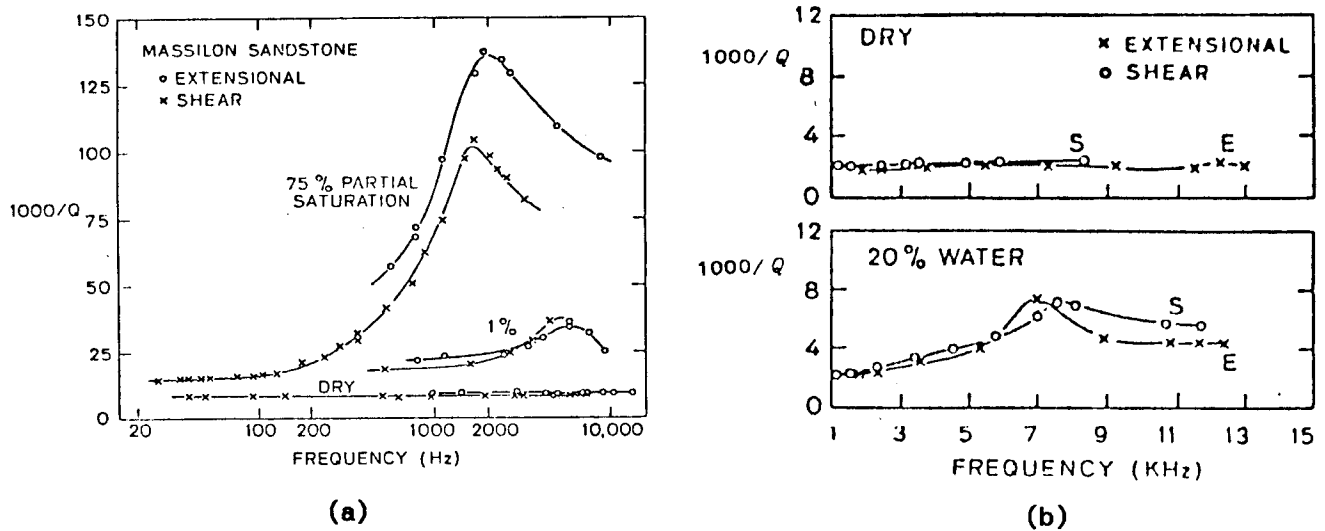


FIG. 1. (a) Quality factor  $Q$  vs. frequency in Massilon sandstone at room pressure and temperature. (b) Measured  $Q$  vs. frequency in vycor porous glass. [Reprinted with permission from Nur, 1980.]

Other physical characteristics of the viscoelastic media must also be discussed in SVSP modeling. In viscoelastic media, seismic phase velocities, reflection coefficients and transmission coefficients all become complex numbers, because attenuation is involved in the wave propagation mechanism. When  $Q$  is assumed to be frequency-independent, the phase velocity,  $c(\omega)$ , is

$$c(\omega) = v_0 \left( \frac{j\omega}{\omega_0} \right)^\gamma, \quad (7)$$

where  $v_0$  is a reference velocity (real number) at reference frequency  $\omega_0$ ,  $j = \sqrt{-1}$ , and  $\gamma$  is a constant given by equation (6) (Nur, 1980).

In the case of a downgoing normal incident wave, the reflection coefficient,  $R_i(\omega)$ , and the transmission coefficient,  $T_i(\omega)$  of interface  $i$ , are

$$R_i(\omega) = \frac{\rho_i c_i(\omega) - \rho_{i+1} c_{i+1}(\omega)}{\rho_i c_i(\omega) + \rho_{i+1} c_{i+1}(\omega)}, \quad (8)$$

$$T_i(\omega) = \frac{2\rho_i c_i(\omega)}{\rho_i c_i(\omega) + \rho_{i+1} c_{i+1}(\omega)}. \quad (9)$$

Because the quality factors of most rocks exceed 10, the value of  $1/Q$  is usually so small that  $\tan^{-1}(1/Q)$  can be replaced by  $1/Q$ . The accuracy of this approximation can be seen in Figure 2. Thus, we can rewrite  $\gamma$  (equation (6)) as

$$\gamma = \frac{1}{\pi Q}. \quad (10)$$

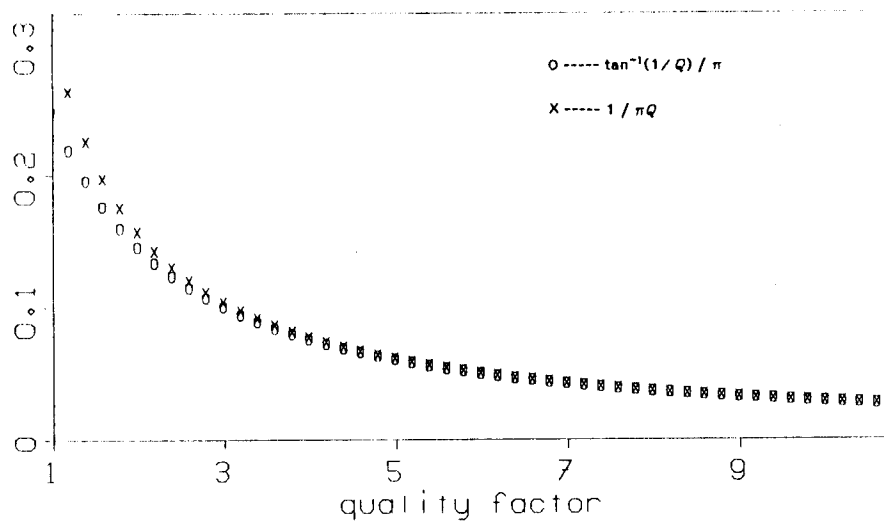


FIG. 2. The curves of  $\tan^{-1}(1/Q) / \pi$  and  $1 / \pi Q$ .

The amplitude of a seismic wave decays exponentially along the ray, this decay can be represented by the following expression:

$$A(\omega) = A_0(\omega) \exp\{-\alpha(\omega)x\}, \quad (11)$$

where  $A(\omega)$  and  $A_0(\omega)$  are the amplitudes at two sites separated by distance  $x$ ,  $\alpha(\omega)$  the attenuation coefficient of the medium. Because the wave's peak energy is proportional to the square of its amplitude, the relative energy lost per cycle, or per wavelength  $\lambda$ , is

$$\frac{\Delta W}{W_0} = \left[ \frac{A_0^2(\omega) - A^2(\omega)}{A_0^2(\omega)} \right]_{x=\lambda} = 1 - \exp\{-2\alpha(\omega)\lambda\}. \quad (12)$$

Equation (12) can be simplified by using Taylor's series expansion and dropping out the higher order terms (because  $\alpha\lambda \ll 1$  for most rocks), so that  $\alpha$  can be related to  $Q$  more explicitly,

$$\frac{\Delta W}{W_0} = 1 - \exp\{-2\alpha(\omega)\lambda\} = 1 - \left\{ 1 - 2\alpha(\omega)\lambda + \frac{1}{2!} [2\alpha(\omega)\lambda]^2 - \dots \right\} = 2\alpha(\omega)\lambda. \quad (13)$$

Because  $W_0$  is the peak energy stored per cycle and is twice the average energy  $W$ , equation (13) can be rewritten as for a sinusoidal signal,

$$\frac{\Delta W}{W} = 2 \frac{\Delta W}{W_0} = 4\alpha(\omega)\lambda. \quad (14)$$

Therefore, the relationship between the attenuation coefficient,  $\alpha(\omega)$ , and the quality factor,  $Q$ , is seen by comparing equations (1) and (14),

$$\alpha(\omega) = \frac{\pi}{\lambda Q} = \frac{\omega}{2v(\omega)Q}, \quad (15)$$

since  $\lambda = 2\pi v(\omega)/\omega$ .

### Transport matrix equations of SVSP

VSP is the seismogram recorded by geophones laid down in a borehole. Both the down-going waves and the upcoming waves are present in a VSP. As shown on Figure 3, these waves across an interface are related by the following expressions (Claerbout, 1976)

$$U'_i(\omega) = [1 - R_i(\omega)] U_{i+1}(\omega) + R_i(\omega) D'_i(\omega), \quad (16-1)$$

$$D_{i+1}(\omega) = -R_i(\omega) U_{i+1}(\omega) + T_i(\omega) D'_i(\omega). \quad (16-2)$$

Equations (16-1) and (16-2) can be rewritten in matrix form,

$$\begin{bmatrix} U'_i(\omega) \\ D'_i(\omega) \end{bmatrix} = \frac{1}{T_i(\omega)} \begin{bmatrix} 1 & R_i(\omega) \\ R_i(\omega) & 1 \end{bmatrix} \begin{bmatrix} U_{i+1}(\omega) \\ D_{i+1}(\omega) \end{bmatrix}. \quad (17)$$

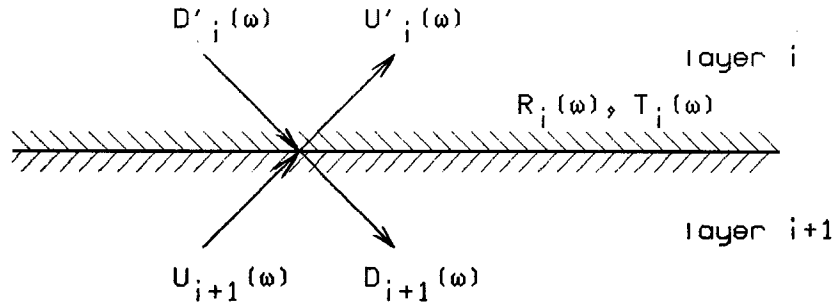


FIG. 3. Waves across an interface.  $D'_i(\omega)$  is the downward incident wave on the interface,  $D_{i+1}(\omega)$  is the downward going wave from the interface,  $U'_i(\omega)$  is the upward coming wave from the interface,  $U_{i+1}(\omega)$  is the upward incident wave on the interface.

To relate the waves at the top and the bottom of one layer, as depicted on Figure 4, both the attenuation factor,  $\exp(-\alpha_i(\omega)\Delta z)$  and the time delay factor,  $\exp(-j\omega\Delta z/v_i)$  must be taken into consideration. The time delay factor,  $\exp(-j\omega\Delta z/v_i)$  is obtained by relating the Fourier transforms of the wave function  $F(t)$  to its delay  $F(t - \Delta z/v_i)$ , because the wave transportation being discussed is in the frequency domain. When the normal incident waves are planar and the subsurface layers are flat, the relationship between waves on both sides of a layer is

$$\begin{bmatrix} U_i(\omega) \\ D_i(\omega) \end{bmatrix} = \begin{bmatrix} e^{-\alpha_i(\omega)\Delta z - j\omega\Delta z/v_i} & 0 \\ 0 & e^{\alpha_i(\omega)\Delta z + j\omega\Delta z/v_i} \end{bmatrix} \begin{bmatrix} U'_i(\omega) \\ D'_i(\omega) \end{bmatrix}. \quad (18)$$

Combining equations (17) and (18) yields the transport matrix equation for layer  $i$  (Ganley, 1981)

$$\begin{bmatrix} U_i(\omega) \\ D_i(\omega) \end{bmatrix} = A_i \begin{bmatrix} U_{i+1}(\omega) \\ D_{i+1}(\omega) \end{bmatrix}, \quad (19)$$

where

$$A_i = \frac{1}{T_i(\omega)} \begin{bmatrix} E_i & E_i R_i(\omega) \\ E_i^* R_i(\omega) & E_i^* \end{bmatrix}, \quad (20)$$

$$E_i = \exp\left\{-\alpha_i(\omega)\Delta z - j\omega\Delta z/v_i(\omega)\right\}, \quad (21-1)$$

$$E_i^* = \exp\left\{\alpha_i(\omega)\Delta z + j\omega\Delta z/v_i(\omega)\right\}. \quad (21-2)$$

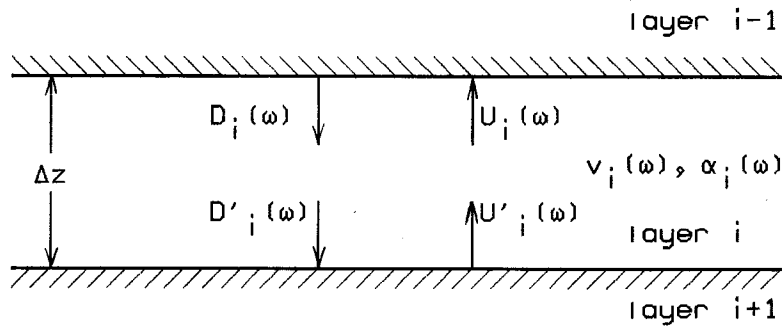


FIG. 4. Waves at top and bottom of a layer.  $\alpha_i(\omega)$  is the attenuation coefficient of layer  $i$ , and  $v_i(\omega)$  the phase velocity of seismic wave in layer  $i$ .

The waves in layer  $i$  and layer  $m$ , ( $i < m$ ), can be related by the expression

$$\begin{bmatrix} U_i(\omega) \\ D_i(\omega) \end{bmatrix} = \prod_{k=i}^{m-1} A_k \begin{bmatrix} U_m(\omega) \\ D_m(\omega) \end{bmatrix}. \quad (22)$$

Equation (22) is called the transport matrix equation characterizing the system of layers from layer  $i$  to layer  $m$ : any two of the four quantities,  $U_i$ ,  $D_i$ ,  $U_m$  and  $D_m$ , can be regarded as the input of the system, while the other two the output.

For a model of  $n$  layers overlying an infinite halfspace, one can write the transport equation as

$$\begin{bmatrix} U_1(\omega) \\ D_1(\omega) \end{bmatrix} = \prod_{k=1}^n A_k \begin{bmatrix} U_{n+1}(\omega) \\ D_{n+1}(\omega) \end{bmatrix}. \quad (23)$$

There is no reflection from the halfspace below, so the upcoming wave  $U_{n+1}(\omega)$  equals zero. On the surface,  $D_1(\omega) = 1 - R_0(\omega)U_1(\omega)$  if the source signal is a delta function generated from beneath the surface. Thus, we have (Ganley, 1981)

$$\begin{bmatrix} U_1(\omega) \\ 1 - R_0(\omega)U_1(\omega) \end{bmatrix} = \prod_{k=1}^n A_k \begin{bmatrix} 0 \\ D_{n+1}(\omega) \end{bmatrix}. \quad (24)$$

After equation (24) has been solved for  $U_1(\omega)$  and  $D_1(\omega)$ , the other upcoming and downgoing waves at any layer can be obtained by the following equation

$$\begin{bmatrix} U_i(\omega) \\ D_i(\omega) \end{bmatrix} = \prod_{k=1}^{i-1} A_k^{-1} \begin{bmatrix} U_1(\omega) \\ D_1(\omega) \end{bmatrix}, \quad (25)$$

where  $A_k^{-1}$  is the inverse of  $A_k$ . The seismogram recorded at depth  $(i-1)\Delta z$ ,  $X_i(\omega)$ , is the sum of the downgoing wave and the upcoming wave at that depth; that is,

$$X_i(\omega) = D_i(\omega) + U_i(\omega). \quad (26)$$

The time section of SVSP at depth  $(i-1)\Delta z$  (trace  $i$ ) can be obtained by the inverse Fourier transform of  $X_i(\omega)$ .

The coefficient matrix,  $A_i$ , is obtained using assumption that only plane waves exist. When the incident wave is spherical or cylindrical, the divergence factor must be incorporated into  $A_i$ . The main contribution of the energy on VSP comes from the downgoing waves, because the reflection coefficients are small compared with the transmission coefficients. Therefore, we can use the divergence factor,  $J_i$ , for the downgoing wave, as an approximation of the total factor of divergence. For a point source,  $J_i$  is given by

$$J_i = \frac{z_{i-1}}{z_i}, \quad (27)$$

where  $z_{i-1}$  is the depth of geophone  $i$ , and  $z_0=1$ . For the line source,  $J_i$  is

$$J_i = \sqrt{\frac{z_{i-1}}{z_i}}. \quad (28)$$

The relationship between  $D_i(\omega)$  and  $D'_i(\omega)$  in equation (18) is, then,  $D_i(\omega) = e^{(\alpha_i(\omega)\Delta z + j\omega\Delta z/v_i)} J_i^{-1}$ . Therefore, the coefficient matrix for non-planar incident wave is,

$$A_i = \frac{1}{T_i(\omega)} \begin{bmatrix} E_i & E_i R_i(\omega) \\ E_i^* R_i(\omega) J_i^{-1} & E_i^* J_i^{-1} \end{bmatrix}. \quad (29)$$

Because the modeling is done in the discrete Fourier domain, the wave energy at the end of the SVSP must be neglectable, if the aliasing problem in the time section of SVSP is to be avoided. Choosing the sample rate of frequency,  $\Delta\omega$ , to be small enough can minimize the aliasing effect. Another limitation in calculating SVSP by the above procedure is that the zero frequency should be replaced by a small number, say  $10^{-8}$ , in computing the zero frequency velocity by equation (7), so that  $T_i(\omega=0)$  is not zero and the transport matrix equation is solvable. Other digital processes such as band-pass filtering and muting (before direct arrivals) have also been incorporated into our program. The program has the option to choose whether the source signal is to be a delta function or a wavelet of decayed



sinusoidal function. When the source wavelet is given, the seismogram can be obtained by convolving the impulse response of the model with the wavelet in time domain, or by multiplying of both spectra in frequency domain.

Figure 5 shows a synthetic VSP seismogram of a four layer model. The reference frequency is 46 Hz, the reference velocities are:  $v_{01}=1500$  meters/sec,  $v_{02}=3000$  meters/sec,  $v_{03}=4000$  meters/sec,  $v_{04}=5000$  meters/sec. The densities are:  $\rho_1=1.5$  g/cm<sup>3</sup>,  $\rho_2=2.0$  g/cm<sup>3</sup>,  $\rho_3=3.0$  g/cm<sup>3</sup>,  $\rho_4=3.5$  g/cm<sup>3</sup>. The quality factors are:  $Q_1=100$ ,  $Q_2=60$ ,  $Q_3=80$ ,  $Q_4=100$ . The thicknesses of layers are:  $z_1=160$  meters,  $z_2=320$  meters,  $z_3=200$  meters. The fourth layer is the halfspace. The first breaks on the figure are direct arrivals, while the reflections and the multiples show up later.

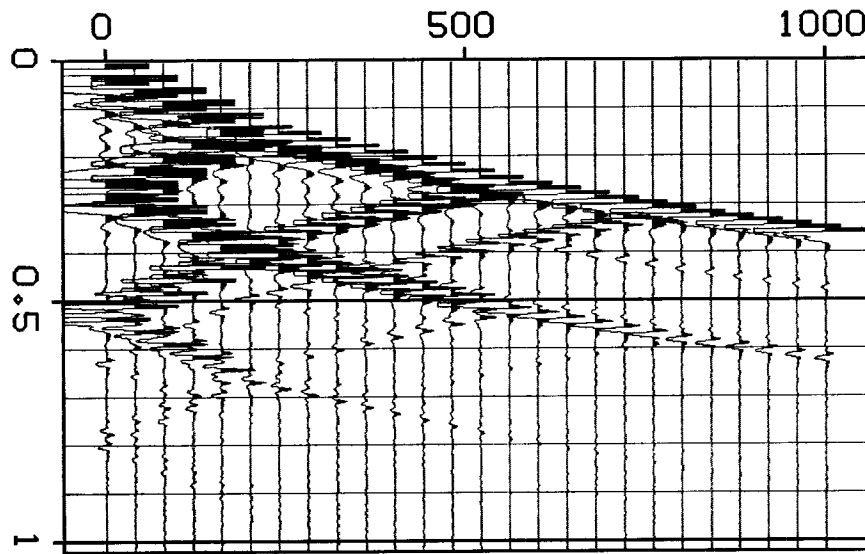


FIG. 5. A SVSP seismogram of a four layer model. Geophones are spaced 40 meters apart in a borehole.

The algorithm for calculating the SVSP is valid even when non-constant  $Q$  models are proposed. Such models require changes only in the subroutine that calculates the parameters such as the phase velocities, the reflection and the transmission coefficients, etc.

**Attenuation and dispersion**

Seismic wave energy decays drastically along the ray path. Most of the energy loss is due to the following factors: geometrical (spherical, or cylindrical) divergence, attenuation, diffraction, reflection, and transmission. Of these factors, the rock attenuation plays an important part in the mechanisms of seismic energy loss. The reflection and the transmission are much less important in the energy decay. Figure 6 shows a three-layer model, with varying values of  $Q$ . Figure 7 shows a comparison between SVSP with a non-attenuation ( $Q=\infty$ ) model and a frequency-independent  $Q$  model; both models otherwise have the same parameters as depicted in Figure 6.

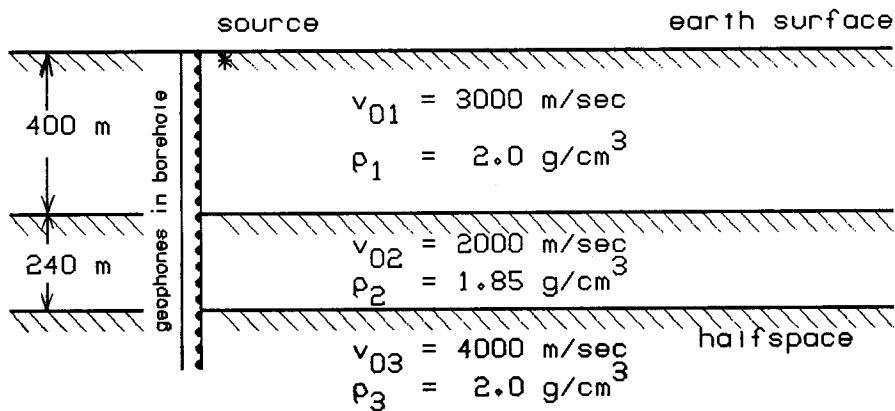


FIG. 6. A three-layer model whose impulse responses are shown in Figure 7. The  $Q$  of the non-attenuation response is infinite. For the attenuated response, the values of  $Q$  are,  $Q_1=100$ ,  $Q_2=50$ ,  $Q_3=100$ .

The phase velocity of seismic wave has the unique relationship (equation (7)) with the attenuation parameter,  $\gamma$ , in the Standard Linear Solid (SLS) model (Nur, 1980). A wave traveling through the SLS media will be distorted, because different frequency components have different velocities and different attenuation coefficients. To show the effects of dispersion, a plot of the waveforms of direct arrivals calculated at different geophone positions within one layer, is shown in Figure 8. The wave spreads out as it travels along.

Seismic attenuation coefficients, velocities, and densities of different rocks can be estimated well by laboratory measurements of rock samples under specified conditions, such as saturation, pressure, and temperature. These parameters used in initial SVSP modeling can be adjusted to match the VSP field data, if the general geology information of the area is available. They can also be used as references for classifying the rock types of the layers, after we have obtained the attenuation coefficients and the velocity distributions

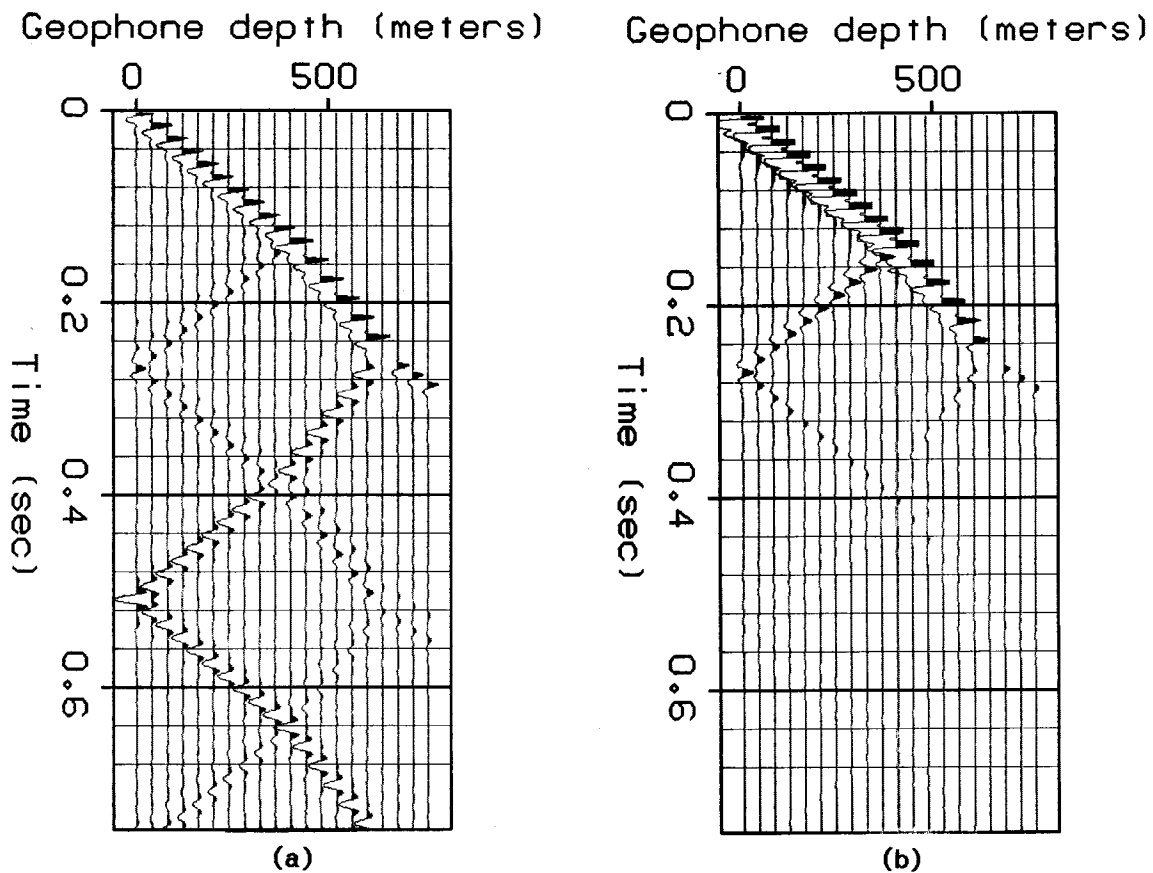


FIG. 7. (a) The non-attenuation SVSP of the model in Figure 6. (b) The SVSP of the same model as (a) with the attenuation parameters specified in Figure 6. Even with the lower plotting clip in (b), the later multiples are so weak that they do not show up in (b) as they do in (a).

from the conventional seismic data processing and the SVSP matching.

### Conclusion

The synthetic VSP can be calculated in the frequency domain; it can incorporate the frequency dependent velocities, attenuation coefficients, reflection and transmission coefficients.  $Q$  is frequency-independent for most rocks over the seismic frequency band.

The effects of seismic attenuation and dispersion have played important roles in analyzing the physical properties of rocks from VSP. The SVSP can be constructed by assuming one set of rock parameters, and reconstructed by comparing the resulting SVSP to the real VSP data. This parameter matching can offer some useful information not only about

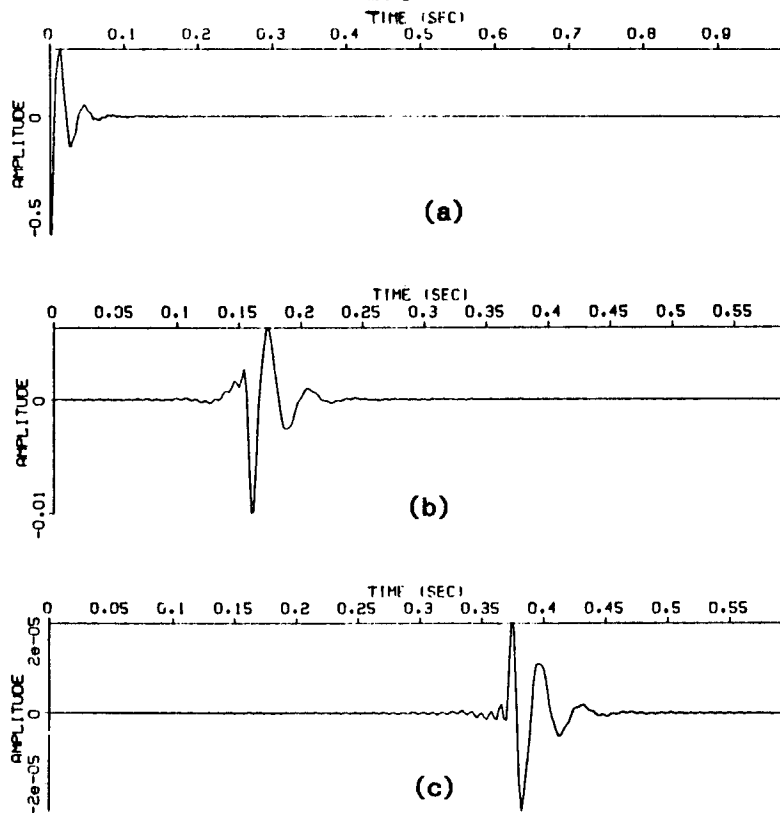


FIG. 8. Waveforms calculated at different geophone positions. The minimum phase source wavelet is shown in (a). The wavelet becomes mixed phased as it travels along.

the structure itself but also about the rock's physical properties.

#### ACKNOWLEDGMENTS

I thank Dr. Tai P. Ng for his helpful suggestions in the work. Special thanks are due to Fanny Toldi, Freelance Editor, for her patient reading and editing of the paper. The author also appreciates the help of Daniel Rothman and Paul Fowler for their reading through the paper.

#### REFERENCES

- Boltzman, L., 1876, Zur Theorie der elastische Nachwirkung: Annalen der Physik und Chemie, *Erganzung*, v.7, p. 624-654.  
 Claerbout, J.F., 1976, Fundamentals of geophysical data processing: New York, McGraw-Hill, Inc.

- Ganley, D. C., 1981, A Method for calculating synthetic seismograms which include the effects of absorption and dispersion: *Geophysics*, v.46, p. 1100-1107.
- Jaeger, J. C., and Cook, N. G. W., 1969, *Fundamentals of rock mechanics*: London, Chapman and Hall.
- Kjartansson, Einar, 1979, *Attenuation of seismic waves in rocks and applications in energy exploration*: SEP 23.
- Nur, Amos, 1980, *Wave propagation in porous rocks*: California, Stanford University.
- O'Connell, R. J., and Budiansky, B., 1978, *Measures of dissipation in viscoelastic media*: *Geophysical Research Letters*, January, 1978.
- White, J.E., 1965, *Seismic waves*: New York, McGraw-Hill Book Company.

# China unwraps micro compatible with IBM PC

BY ALEXANDER BESHER

Contributor

**J**ust when it appeared that all the IBM PC-compatible computers had come out of the woodwork, a new compatible has been announced by the People's Republic of China (PRC).

The Great Wall 100 is a 16-bit machine that has been developed by the Beijing Research Institute of Electronic Application in cooperation with the Beijing Wire Communications Plant, which is actually manufacturing the computers. Both firms are government owned and operated.

But IBM need not lose any sleep over the Great Wall just yet. Only 1000 models have been shipped so far, and the price of the PRC personal computer is still far from competitive at 30,000 yuan (approximately \$15,000 in U.S. currency).

Although the Great Wall 100 comes equipped with a game joystick and control panels, it's not likely to become a source of entertainment for the vast majority of Chinese families, who can ill afford to buy the machines. Chinese officials say they are developing application software to address their country's most immediate and pressing needs in such areas as agriculture, water-power projects, meteorology, construction, medicine, machine building, mining, railways, the textile industry and national defense.

The Chinese claim their machine has complete compatibility with IBM PC software, since the Great Wall 100 will reportedly run the MS-DOS, CP/M-86 and UCSD p-System operating systems as well as Oasis and QNXI. The standard Great Wall 100 comes with the newly developed Chinese character disk operating system (CCDOS), so that Chinese characters can be used in various high-level languages that are supported by CCDOS. A two-level simplified Chinese-character library with over 7000 Chinese characters is stored on the floppy disk and can be called into the main memory in less than 20 seconds.

The Great Wall can also communicate with a mainframe and has the capability of hooking up with a local-area network. The local-area network is still being developed by Qinhua University in Beijing and is expected to be operational in 1984.

The Great Wall 100 comes with a 4.77 MHz 8088 microprocessor; 256K RAM,

which is expandable to 512K; 40K ROM; two 320K, 5¼-inch floppy disk drives (two additional floppies are also available); a high-resolution green-phosphor display; and a parallel-printer adapter. The machine's main memory can be expanded to 1 megabyte, and a 8087 math processor can be incorporated with the central Intel 8088 processor.

The Chinese are in the process of converting a number of popular American application software packages — including data-base management, word processing, statistics, finance and accounting and graphics programs — into Chinese for the

Great Wall 100.

Instruction manuals come in both English and in Chinese, so apparently the Chinese are not ruling out the possibility of selling the Great Wall 100 in the West once they've geared up production of the machine.

As the sales brochure states, "Great Wall 100 will remain in the forefront of modern microcomputers and become the most faithful and capable assistant of yours. You are welcome to use the Great Wall 100."

Manufacture of the Great Wall 100 comes on the heels of the Reagan Administration's announcement last November of more liberalized trade restrictions on high-technology exports to China than in the past. Among the items expected to get export clearance much more quickly are microcomputer systems. ●

*Alexander Beshar is a free-lance writer who recently returned from an assignment in the People's Republic of China.*